Proceedings of the
44th IEEE Conference on Decision and Control, and
the European Control Conference 2005
Seville, Spain, December 12-15, 2005

On Complexity Reduction of Voltage Stabilization MPC Schemes by Partial Explicit Feedbacks

Sid Ahmed Attia and Mazen Alamir

Abstract— **In this paper, voltage stabilization of power systems is considered. The proposed control approach relies on using local feedback strategies to update the OLTC setpoints and a receding horizon global controller to update the reactive power injections and load shedding. The combinatorics associated with the capacitors and load shedding discrete inputs are partially alleviated by using an efficient parametrization and ordering techniques. Simulations are carried out on a benchmark power system to further illustrate the approach.**

Index Terms— **voltage stability, model predictive control, efficient open loop parametrization, combinatorial optimization, local OLTC feedback**

I. INTRODUCTION

In the last decade, the power community has shown a great interest in systematic design methods for assessing stability in power networks. Voltage instability is undeniably one of the costliest power systems failures. For instance, the 14 August 2003 blackout in North America cost between US $4 billion and $6 billion [1]. Basic material on voltage stability may be found in the recent survey [2] and the references therein.

Much of the work reported on voltage collapse mitigation relies on strong knowledge of the power system. Basically, the experience gained by the designers is put forward. Schemes such as those developed in e.g., [3] where heuristics based load shedding strategies are compared with branch and bound based ones. The multi step design consist in time domain simulation for generating training scenarios. An optimization stage is then carried out to minimize the amount of load shedding with respect to the value found in the training set.

Another family of methods relies on computing a security margin or a distance to voltage collapse, see e.g., [4] for a survey of the main indices. Based on these measures, sensitivities with respect to the different control actions are computed. These provide directions towards which the control is updated, this is in general followed by a constrained multiple optimization stage for dispatching the different control actions, see e.g., [5]. In the same spirit, the authors in [6] use a quasi steady state simulation approach. A simple formula is then proposed to update the different control actions based on off line bus ranking. In [7] a clear distinction is made between the different control actions. A scheme is then derived where a corrective and a preventive control strategies interact, the first is used in extreme contingencies (loss of system solvability) while the latter is for enhancing the system stability margin.

The method developed in this paper fall into the category where only knowledge of the power system model is needed. This model should incorporate at least the dominant features i.e., the load dynamics since voltage collapse is driven by these dynamics. These approaches include mainly methods based on predicting and analyzing sensitivities of the system trajectories see e.g., [8] where this is discussed in the more general framework of hybrid systems. The predictive control approach has been first exploited in the leading paper [9]. The approach is further improved in subsequent work by the same authors in [10] where techniques from Artificial Intelligence are used as alternatives to further reduce the combinatorics. Basic material on predictive control can be found in the survey [11].

The aim of the present paper is to explore a particular controller design methodology for voltage collapse avoidance in power systems. The emphasis is put on a benchmark problem [12]. This is a step towards a fully coordinated decentralized solution in the spirit of [13]. The focus here is on the area central controller. We will not deal with the higher level authority used to coordinate areas controllers. Indeed, we believe that at a higher level an expert system with advanced heuristics shall be used. The proposed approach relies on a decomposition strategy. The power system is decomposed into regions, in each region a local controller is implemented to update the internal variables i.e., the OLTC setpoints. At the higher level a global predictive strategy is in force to activate the reactive power injections and load shedding. At this stage, a simple open loop parametrization together with an efficient ordering technique are proposed to alleviate the associated combinatorics.

II. BENCHMARK PRESENTATION

The following section is a brief presentation of the ABB medium scale benchmark (a small test system in the absolute), the reader is referred to [12] for a detailed description. The power system motivating the study is the one depicted in figure 1. It is composed of the following elements

- Two generation elements G_1 and G_2.
- An infinite bus, used to represent the rest of the network.
- Three interconnected areas represented by the *area* elements.

This work was partially supported by the European Project Control & Computation IST-2001-33520

M. Alamir is with Laboratoire d'Automatique de Grenoble, Domaine Universitaire BP46-38402 Saint Martin d'Hères, France Mazen.Alamir@inpg.fr

S. A. Attia is on leave from the Laboratoire d'Automatique de Grenoble, attia@ieee.org

0-7803-9568-9/05/$20.00 ©2005 IEEE

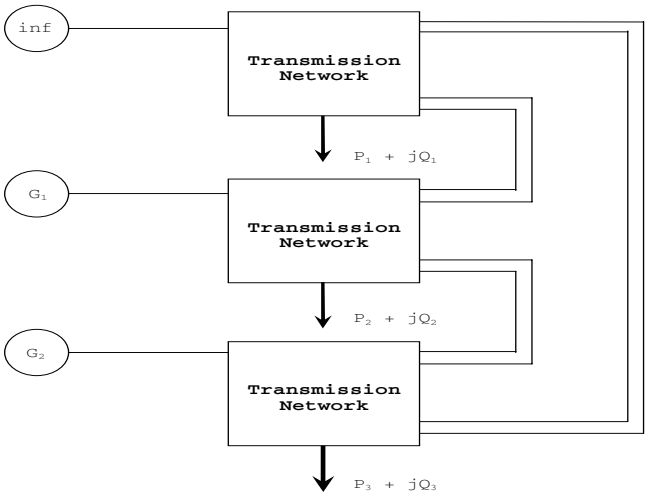

Fig. 1. The ABB medium scale benchmark

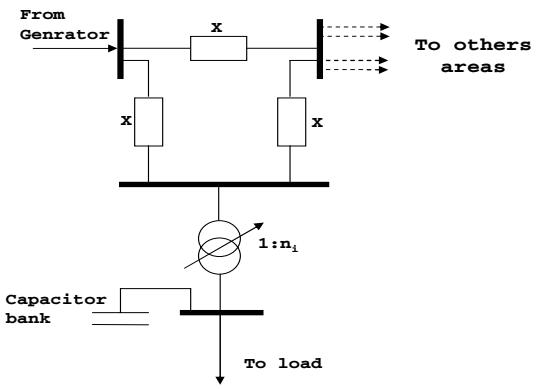

Fig. 2. Transmission network in the ABB medium scale benchmark

- Three double transmission lines modelled as pure reactances, denoted as $X_{i_1 i_2}^{i_3}$ where the subscripts i_1 and i_2 refer respectively to the departure and arrival areas and the superscript i_3 the line index $i_3 = 1, 2$. Due to inter-area faults, these parameters may undergo sudden changes.

In figure 2 is depicted the content of the transmission network bloc. Initially a network of this type was proposed as a benchmark. Solutions were then proposed by the different project partners. In [14] the nonlinear hybrid dynamics are converted to a Mixed Logical Dynamical system by finely approximating the nonlinearities. A predictive control strategy is then developed only to update the transformer turn ratio. On the contrary no preliminary (time-consuming) approximation stage is required for the approach developed in [15] where an efficient open loop parametrization is shown to give satisfactory results with highly reasonable computation times.

The area block is composed of the following components

- Three transmission lines modelled as constant pure reactances X.
- A transformer equipped with an *On Load Tap Changer* OLTC. The state graph in Figure 3 illustrates the function of a typical OLTC control system. The automata has three possible states labelled as, *Wait*, *Count* and *Action* state
  - Wait state: the automata is in this state as long as the condition $|v_i - v_{r_i}| \leq \Delta$ is satisfied where v_{r_i} is the continuous control input to the OLTC, v_i the load voltage, Δ is a positive real threshold and i is the area index $i \in \mathcal{I} = \{1, \ldots, l\}$ ($l = 3$ for the case study)
  - Count state: while the automata is in this state, a timer T_{count} is activated and if it exceeds a certain value T_d (typically $30sec$), the automata passes to the next action state
  - Action state: a control action is taken, the turn ratio n_i is one-step increased (decreased) if the threshold Δ ($-\Delta$) is exceeded (not exceeded), i.e.,

$$n_i^+ = \begin{array}{lll} n_i^- + dn & \text{if } v_{r_i} - v_i > \Delta & \text{and } n_i^- < n_{max} \\ n_i^- - dn & \text{if } v_{r_i} - v_i < -\Delta & \text{and } n_i^- > n_{min} \end{array} \quad (1)$$

where the superscript $-$ and $+$ represent respectively the instants just before and after the update, dn is the turn ratio increment ($dn = 0.02$), n_{max} and n_{min} are respectively the maximal and minimal value of the turn ratio

- A reactive power source represented by the capacitor bank b_i. This is actually the second control input to the area network.
- A nonlinear load with recovery dynamics described by the following first order differential equation [12]

$$T_{p_i} \dot{x}_i + x_i = P_s(v_i) - P_t(v_i) \quad (2)$$

where x_i is the $i-th$ load internal state, T_{p_i} the recovery time constant, $P_s(v_i) = P_{0_i} v_i^{\alpha_s}$ and $P_t(v_i) = P_{0_i} v_i^{\alpha_t}$ are respectively the steady state and transient voltage dependencies, P_{0_i} is the steady state active power. The absorbed active and reactive power can be written as

$$P_i = (1 - k_i) \left(-\frac{x_i}{T_{p_i}} + P_t(v_i) \right) \quad (3)$$

$$Q_i = (1 - k_i) (\alpha_i P_i) \quad (4)$$

$\alpha_i = cst_i$ is the constant power factor. The variable k_i represents the load shedding percentage, allowing a higher level controller to disconnect a part of the load. Actually, the third control input to the area block.
The control inputs can be grouped in the following continuously valued vector

$$u_c = (v_{r_1} \ldots v_{r_l})^T \quad (5)$$

and discretely valued one

$$u_d = (b^T \ k^T)^T \tag{6}$$

with $b^T = (b_1 \dots b_l)$, $k^T = (k_1 \dots, k_l)$. The power system can thus be written in a compact *Differential Algebraic Equation* form

$$\dot{x} = f(x, v, \theta) \tag{7}$$
$$0 = g(x, v, \theta, u_c, u_d) \tag{8}$$

where $x = (x_1, \dots, x_l)$ is the states vector and $v = (v_1, \dots, v_l)$ is the loads voltage vector, θ groups the different network parameters i.e., lines reactance among others. The vector field f describes the load dynamics and g the network topology (power flow equations).

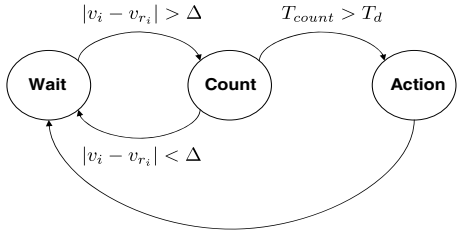

Fig. 3. The OLTC dynamics

A. Complexity of a Full Predictive Control Solution

Nonlinear predictive control is now widely recognized to be a feedback strategy providing a relatively easy handling of both nonlinearities, constraints and optimality concerns. Recall that predictive control schemes amount to compute at each sampling time jT_s (j is a nonnegative integer and T_s is the sampling period) an optimal open-loop control sequence (in the sense of some given cost functional), to apply the first part of the resulting optimal open-loop control sequence until the next sampling instant. At the next sampling instant, the whole problem is re-considered on a moving-horizon basis and the procedure is repeated resulting in a state feedback law. For long prediction horizons N_pT_s ($N_p \in \mathbb{Z}^+$), this may lead to open loop optimal control problems with a high dimension of the decision variable. In fact this is the case for the problem under study. To illustrate further, let us consider the general case where l similar areas are interconnected. Suppose that all of these regions are equipped with the same control elements b_i and k_i under the following constraints

$$k_i \in \mathcal{K} = \{0, 1, \dots k_{max}\}, \quad i \in \mathcal{I} = \{1, \dots, l\} \tag{9}$$
$$b_i \in \mathcal{B} = \{0, 1, \dots b_{max}\} \tag{10}$$

since the state automata describing the OLTC is invertible, one can consider directly that the control input to the power system is the transformer turn ratio n_i [15], [14] since only three moves are allowed (see Equation (1)). The complexity of a receding horizon approach for a fixed prediction horizon N_p is bounded by the following

$$\mathcal{C}_{full} = [3 \times (k_{max} + 1) \times (b_{max} + 1)]^{l \times N_p} \tag{11}$$

for the benchmark under consideration, $k_{max} = 2$, $b_{max} = 1$ and $l = 3$, this gives the upper bound $18^{3 \times N_p}$.

The complexity can be reduced (or more exactly distributed) by introducing explicit feedback strategies to update some internal variables. In this contribution a simple feedback law is introduced to update the voltage reference to the OLTC. The feedback is based on a direct inversion of the discrete dynamics and on the assumption that the transformer turn ratio is solely used to enhance the power system voltage level. For other purposes, more advanced heuristics or analytical design can be used.

This has the drastic effect to reduce the complexity $\mathcal{C}_{full}$ by a factor of $3^{l \times N_p}$, giving the following complexity

$$\mathcal{C}_1 = [(k_{max} + 1) \times (b_{max} + 1)]^{l \times N_p} \tag{12}$$

that is still dependent on the prediction horizon N_p. Next, an open loop control parametrization together with an efficient ordering technique are introduced to further reduce the combinatorics. The control approach is detailed in the next section.

III. THE CONTROL APPROACH

A. A Local Feedback Strategy

The local feedback strategy developed in this work is used as a voltage enhancement control action. This means that it is only introduced to enhance the stability level of the power system (achieves a higher equilibrium), not to restore it. In conjunction with this, a global predictive strategy is used as a corrective action (restores a lost equilibrium) for updating the capacitor and load shedding values. Indeed the corrective action allows the movement of unsolvable point (voltage collapse) to the closest equilibrium, then the tap changer action is used to achieve a higher stability level. The assumption that the sensitivity matrix with respect to the tap positions is positive definite then follows [16] and is used next to derive the local scheme.
Starting with the update equations of the OLTC

$$n_i^+ = \begin{cases} n_i^- + dn & if \ v_{r_i} - v_i > \Delta \quad and \ n_i^- < n_{max} \\ n_i^- - dn & if \ v_{r_i} - v_i < -\Delta \quad and \ n_i^- > n_{min} \end{cases} \tag{13}$$

In order to increase the load voltage, one needs to increase the value of the turn ratio n_i. It is then sufficient to take for v_{r_i}

$$v_{r_i} = (v_i + \Gamma\Delta), \quad \Gamma > 1 \tag{14}$$

to make active the first part of (13). The same reasoning, leads for the case where a voltage decrease is needed to the following

$$v_{r_i} = (v_i - \Gamma\Delta) \tag{15}$$

By combining equations (14)-(15) and introducing an exogenous signal v_i^* the following update equation is obtained

$$v_{r_i} = (v_i + \Gamma\Delta sgn(v_i^* - v_i)) \tag{16}$$

where v_i^* is a voltage target equilibrium associated with the $i-th$ area and $sgn(\cdot)$ is the usual sign function.

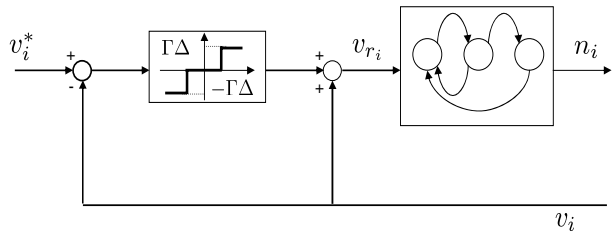

Fig. 4. The local feedback strategy for updating the OLTC reference

The target voltage v_i^* needs not be a true equilibrium of the system (a true equilibrium will need a preliminary power flow analysis, not necessary in this case). Thus, in most cases exact tracking of v_i^* can not be achieved. A dead zone is then introduced i.e., the value of the turn ratio is blocked whenever the voltage enters the dead zone. The bloc diagram is shown in figure 4.

Recall here that a more sophisticated scheme is to use a feedback from exogenous signals to increase the dead zone or flip it whenever respectively tap locking or reversing is required (this is a consequence of a non positive definite sensitivity matrix). This scheme will thus be useful if the local controller is used as a corrective control action see e.g., [17] and [18].

B. The Predictive Control Strategy

In this section, we present the global feedback strategy used to update the values of the capacitor bank and load shedding. Let us consider a power system composed of l areas. Each area is indexed from 1 to l and equally equipped with a capacitor bank b_i and load shedding mechanism k_i

$$\begin{aligned} k_i \in \mathcal{K} &= \{0,1,\dots k_{max}\}, \quad i \in \mathcal{I} = \{1,\dots,l\} \quad (17) \\ b_i \in \mathcal{B} &= \{0,1,\dots b_{max}\} \quad (18) \end{aligned}$$

let us briefly recall some of the notation, b, k and v denote respectively the vectors of capacitor values $(b_1,\dots b_l)^T$, load shedding $(k_1,\dots k_l)^T$ and load voltages $(v_1,\dots v_l)^T$. The control input vector is $u_d^T = (b^T, k^T)$. The control is implemented in a discrete scheme with a sampling period $T_s = T_d$ (the counter threshold in the OLTC), the control input is given at each sampling instant jT_d where j is a nonnegative integer as

$$u_d(j) = \begin{pmatrix} b(j) \\ k(j) \end{pmatrix} \in \mathcal{B}^l \times \mathcal{K}^l \quad (19)$$

where the sets $\mathcal{B}$ and $\mathcal{K}$ are defined as above. Let $\tilde{u}_d(j)$ denotes the open loop control profile at the instant jT_d over the prediction horizon N_p

$$\tilde{u}_d(j) = (u_d(jT_d),\dots,u_d((j+N_p-1)T_d)) \quad (20)$$

let us also denote by $\mathcal{U}_d$ the set of admissible open loop control profiles, then the following set of constant admissible profiles is introduced as

$$\mathcal{U}_d^{(\bar{b},\bar{k})} = \{\tilde{u}_d \in \mathcal{U}_d \mid \tilde{u}_d \equiv (\bar{b},\bar{k})\} \quad (21)$$

where $(\bar{b},\bar{k}) \in \mathcal{B}^l \times \mathcal{K}^l$. Let us also define the set of load shedding vectors with equal components as

$$\mathcal{K}_o = \{\bar{k} \in \mathcal{K}^l \mid \bar{k}_1 = \bar{k}_2 = \dots = \bar{k}_l\} \quad (22)$$

meaning that load shedding is equally distributed among the areas, and that they are equally treated (in percentage, not in the absolute quantities, see also remark 1). An ordering map can now be defined on the set $\mathcal{K}_o$ as

$$\mathcal{O} : \mathcal{K}_o \longrightarrow \{1,2,\dots,card(\mathcal{K})\} \quad (23)$$

such that

$$\{\bar{k}^{(1)} \geq \bar{k}^{(2)}\} \Longleftrightarrow \left\{\mathcal{O}(\bar{k}^{(1)}) \geq \mathcal{O}(\bar{k}^{(2)})\right\} \quad (24)$$

Let the set $\mathcal{S}_{nc}$

$$\begin{aligned} \mathcal{S}_{nc} = \Big\{ &(\bar{b},\bar{k}) \in \mathcal{B}^l \times \mathcal{K}_o \mid \forall \tilde{u}_d \in \mathcal{U}_d^{(\bar{b},\bar{k})} \ : \\ &v(\cdot;x_0,\tilde{u}_d) \text{ is defined over } [0 \ N_pT_d] \Big\} \end{aligned} \quad (25)$$

be defined as the set of capacitors and load shedding vector such that *no voltage collapse is induced* (no singularity happens over the prediction horizon). Here $v(\cdot;x_0,\tilde{u}_d)$ represents the load voltages vector under the constant profile $\tilde{u}_d$ and the load states initial condition $x_0 = x(0)$. Next a subset of $\mathcal{S}_{nc}$ is defined as

$$\begin{aligned} \mathcal{S}_f = \{&(\bar{b},\bar{k}^*) \in \mathcal{S}_{nc} \mid \\ &\bar{k}^* = \arg \min_{\bar{k} \in \mathcal{K}_o, \exists \tilde{u}_d \in \mathcal{U}_d^{(\bar{b},\bar{k}^*)}, \ v(N_pT_d;x_0,\tilde{u}_d) > \underline{v}} \mathcal{O}(\bar{k})\} \end{aligned} \quad (26)$$

as the set of capacitors with minimum load shedding such that a final constraint on the load voltages is fulfilled, where $v(N_pT_d;x_0,\tilde{u}_d)$ represents the voltage vector at the final prediction instant N_pT_d. Note the value of minimum load shedding can be different in the two sets $\mathcal{S}_{nc}$ and $\mathcal{S}_f$ as defined in (25)-(26) and that $\mathcal{S}_f \subseteq \mathcal{S}_{nc}$ since the control pair that satisfies the terminal inequality does not induce a voltage collapse.

The following quadratic performance measure is then introduced

$$J = \int_0^{N_pT_d} (v(\tau) - v_{ref})^T P (v(\tau) - v_{ref}) d\tau \quad (27)$$

where P is a positive definite matrix of appropriate dimensions and v_{ref} is a vector containing the voltage references to the power system. Note here that no penalty terms are needed neither on the control inputs nor on the terminal voltages since respectively an ordering map (23) is already in force and a terminal inequality is embedded in (26). Taking constant open loop control profiles leads to a complexity that is independent of the prediction horizon.

The full complexity $\mathcal{C}_{full}$ is further reduced by a factor of $[(k_{max}+1)\times(b_{max}+1)]^{N_p}$ leading to the following

$$\mathcal{C}_2 = [(k_{max}+1)\times(b_{max}+1)]^{l} \tag{28}$$

Remark 1: In the final algorithm, a lower level optimization stage is introduced to further discriminate between the components of the load shedding vector i.e., the regions. This yields a coordinated load shedding strategy which can be effective in stopping cascaded outages in contrast to approaches based on only shedding load in the region where the fault is.

Remark 2: A key feature in receding-horizon control is that the resulting closed-loop control is much more rich than the underlying open-loop parametrization. The consequence of this is that in many cases, apparently over-simplified open-loop parameterizations results in a sufficiently rich closed-loop control behavior.

C. The Control Algorithm and its complexity

Next, the control algorithm together with an efficient ordering technique are summarized. The main steps are as follows

Step 1 Compute the set $\mathcal{S}_{nc}$ of capacitors $\bar{b} \in \mathcal{B}^l$ with minimum load shedding $\bar{k}^* \in \mathcal{K}_o$ such that no voltage collapse occurs during the prediction horizon N_p.

Step 2 Compute the set $\mathcal{S}_f \subseteq \mathcal{S}_{nc}$ such that the voltages at the terminal prediction horizon satisfy the constraint $v(N_pT_d;\cdot,\cdot) \geq \underline{v}$.

Step 3 Among all the possibilities compute the minimum of the performance index J in $\mathcal{S}_{nc}$ **if** $\mathcal{S}_f = \emptyset$ **else** in $\mathcal{S}_f$. Denote the minimizing pair by $(\bar{b}^*, \bar{k}^*)$.

Step 4 $s := l-1$, $D := \{1,\ldots,l\}$

Step 5 **if** $(\min_{i\in D}(\bar{k}_i^*) \neq 0))$ **then**

- Generate all the vectors $\bar{k}$ such that at most s components $\bar{k}_i$ $(i \in D)$ are decreased by 1 with respect to the corresponding component $\bar{k}_i^*$
- Compute if any the argument minimizing the performance index J over the set of vectors $\bar{k}$ generated so far, that guarantee constraint satisfaction on the terminal voltages $v(N_pT_d;\cdot,\cdot)$. **If** such a vector does not exist **then** Goto **Step 6 else** denote it as $\bar{k}^{**}$ **end if**
- Compute the set D of components indices of $\bar{k}^{**}$ and $\bar{k}^*$ that disagree, $D := \{i \in \{1,\ldots,l\} : \bar{k}_i^{**} \neq \bar{k}_i^*\}$ (this set contains indices of components that can be decreased at the next iteration of $step$ 5)
- $\bar{k}^* := \bar{k}^{**}$, $s := card(D)$ Goto **Step 5**

end if

Step 6 Apply $(\bar{b}^*, \bar{k}^*)$ and Goto **Step 1**.

Remark 3: In $step$ 5 of the algorithm, only the vectors with a number of different components at most equal $l-1$ are generated (at the first iteration in $step$ 5). Indeed, generation of vectors with full distance (l) is not required since all the vectors in $\mathcal{K}_o$ are tested before entering $step$ 5.

In $step$ 1, the set $\mathcal{S}_{nc}$ is computed by a simple enumeration. This enumeration needs

$$\mathcal{C}_{step1} = card(\mathcal{B})^l \times card(\mathcal{K}_o) \tag{29}$$

evaluations at most over the prediction horizon (since the open loop control profiles are taken constant). The $step$ 2 needs no particular computations since the inclusion relation $\mathcal{S}_f \subseteq \mathcal{S}_{nc}$ is satisfied all the time, therefore computing $\mathcal{S}_f$ amounts at checking the values inducing satisfaction of the final penalty constraint. $step$ 3 needs a direct comparison of at most $\mathcal{C}_{step1}$ values of the performance index J. $step$ 5 generates all the vectors such that s components $\bar{k}_i$ $(i \in D)$ are decreased by 1 with respect to the corresponding component $\bar{k}_i^*$.

The complexity in terms of visited nodes in the general case is at most

$$\mathcal{C}_3 \quad = \quad (\bar{k}_i^*+1)(2^{l-1}-1) \tag{30}$$

instead of

$$\mathcal{C} = (\bar{k}_i^*+1)^l \tag{31}$$

for an exhaustive exploration, where $\bar{k}_i^*$ is any component of the vector $\bar{k}^*$ at the first stage.

IV. SIMULATION RESULTS

Next, extensive simulation results are reported for different realistic operating conditions of the power system. From the time constants of the power system [12], one can infer the approximate value of the prediction horizon such that the dynamics are captured. In all the closed loop simulation results, this value is taken as $N_p = 10$ $(300\ sec)$. All the simulated faults reported next induce a voltage collapse in the absence of appropriate controller, and thus correspond to extreme operating conditions. The faults are discriminated by using an integer valued vector $F = [f_1\ f_2\ f_3]$ that takes its values $f_i \in \{0,1,2\}$ corresponding to outage of none, one or both of the lines connecting the areas. Provided that the integration of the model over the prediction horizon is under $\frac{T_s}{\mathcal{C}_{step1}\mathcal{C}_3}$ the approach can be implemented in real time fashion (with the help of efficient simulation techniques), since $step$ 5 consists in an efficient enumeration technique that is a 'less consuming' operation ($\approx \frac{T_s}{110}$).

V. CONCLUSIONS

In this contribution, a predictive control strategy is proposed for voltage stabilization in power systems. The approach uses local feedback strategies to update the OLTC's set points together with a simple open loop parametrization to alleviate the combinatorics associated with the discrete inputs. Extensive simulation results are reported for a benchmark power system showing the applicability of such a scheme (see the extended version [19]). Future work concerns the case of larger scale systems. The proposed control strategy will then be used as an agent. The whole architecture will be of a decentralized type with some of the information flow centralized in a higher coordinating authority.

REFERENCES

[1] P. Fairley. The unruly power grid. *IEEE Spectrum*, Aug 2004.

[2] T. Van Cutsem. Voltage instability : Phenomena, countermeasures and analysis methods. *Proc. of the IEEE*, 88(2):208–227, Feb 2000.

[3] T. Van Cutsem, C. Moors, and D. Lefebvre. Design of load shedding schemes against voltage instability using combinatorial optimization. In *IEEE Power Eng. Soc. Win. Meet.*, pages 848–853, 27-31 Jan 2002.

[4] C.A. Canizares, A.C.Z. De Souza, and V.H. Quintana. Comparison of performance indices for detection of proximity to voltage collapse. *IEEE Trans. on Pow. Syst.*, 11(3):1441–1450, Aug 1996.

[5] Q. Wu, D. H. Popovic, D. J. Hill, and C. J. Parker. Voltage security enhancement via coordinated control. *IEEE Trans. on Pow. Syst.*, 16(1):127–135, Feb. 2001.

[6] T. Van Cutsem, Y. Jacquemart, J. N. Marquet, and P. Pruvot. A comprehensive analysis of mid-term voltage stability. *IEEE Trans. on Pow. Syst.*, 10(3):1173–1182, Aug 1995.

[7] Z. Feng, V. Ajjarapu, and D. J. Maratukulam. A comprehensive approach for preventive and corrective control to mitigate voltage collapse. *IEEE Trans. on Pow. Syst.*, 15(2):791–797, May 2000.

[8] I. Hiskens and M. A. Pai. Trajectory sensitivity analysis of hybrid systems. *IEEE Trans. on Cir. and Sys.*, 47(2):204–220, Feb 2000.

[9] M. Larsson, D. J. Hill, and G. Olsson. Emergency voltage control using search and predictive control. *Int. Jour. of Elect. Pow. & Ener. Syst.*, 24(2):121–130, Feb 2002.

[10] M. Larsson. A model-predictive approach to emergency voltage control in electrical power systems. In *43rd IEEE CDC*, pages 2016–2022, Paradise Island, Bahamas, Dec 2004.

[11] D. Q. Mayne, J. B. Rawlings, C. V. Rao, and P. O. Scokaert. Constrained model predictive control: Stability and optimality. *Automatica*, 36:789–814, 2000.

[12] M. Larsson. The abb medium scale power transmission test case. Technical report, ABB, http://www.dii.unisi.it/ hybrid/cc/, Feb 2004.

[13] B. Fardanesh. Future trends in power system control. *IEEE Comp. Appl. in Power*, pages 24–31, Jul 2002.

[14] T. Geyer, M. Larsson, and M. Morari. Hybrid emergency voltage control in power systems. In *ECC*, UK, 2003.

[15] S. A. Attia, M. Alamir, and C. Canudas de Wit. Voltage collapse avoidance in power systems : A receding horizon approach. *To be published in Special Issue of the Int. Jour. Autosoft*, 2005.

[16] V. Venkatasubramanian, H. Schättler, and J. Zaborsky. Analysis of the tap changer related voltage collapse phenomena for the large electric power system. In *31st IEEE CDC*, pages 2920–2927, Arizona, Dec 1992.

[17] C. Vournas and M. Karystianos. Load tap changers in emergency and preventive voltage stability control. *IEEE Trans. on Pow. Syst.*, 19(1):492–498, Feb 2004.

[18] S. Solyom, B. Lincoln, and A. Rantzer. A novel method for voltage stability control in power systems. In *6th World Automation Congress*, Sevilla, Spain, Jul 2004.

[19] S. A. Attia and M. Alamir. A model predictive control scheme for voltage stabilization in power systems. *Submitted to the IEEE*, 2005.

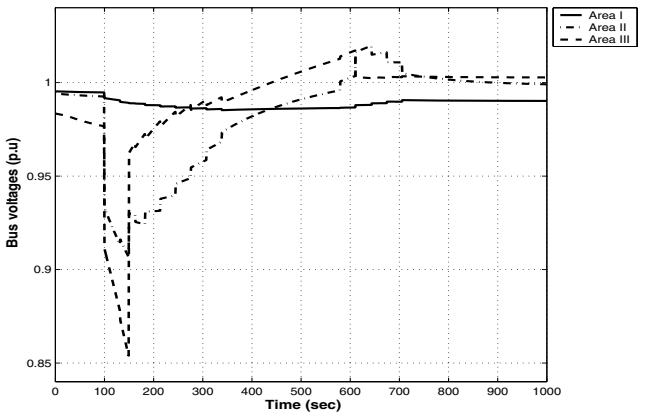

Fig. 5. Load voltages under the fault [0 1 2] and closed loop control

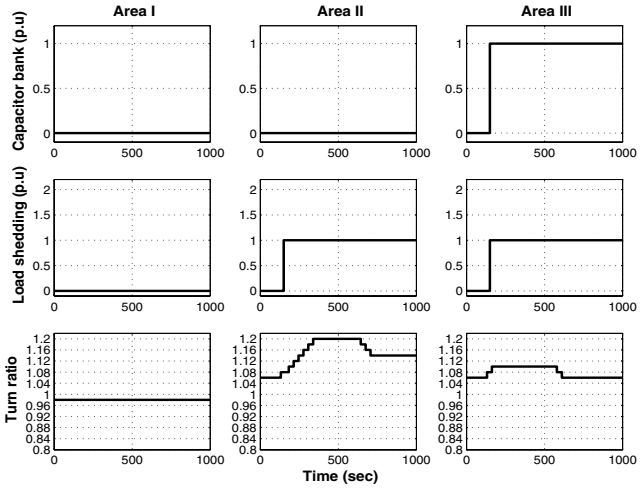

Fig. 6. Control inputs under the fault [0 1 2]

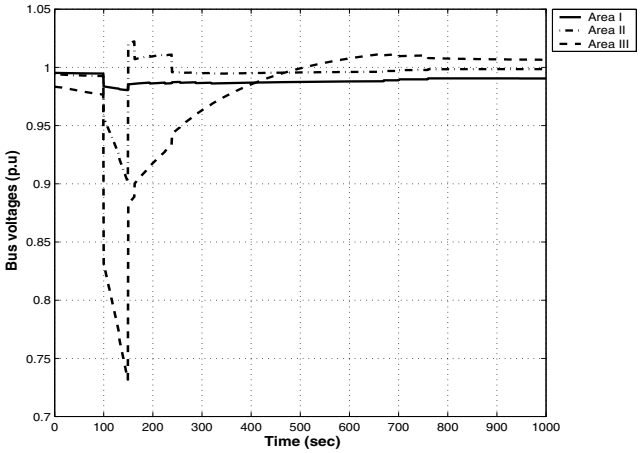

Fig. 7. Load voltages under the fault [2 1 0] and closed loop control

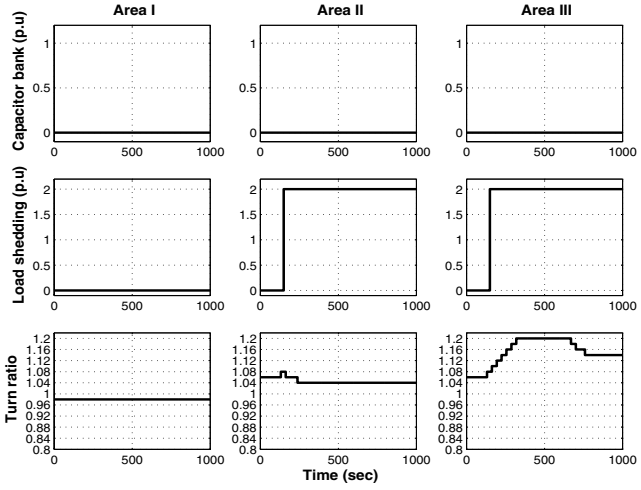

Fig. 8. Control inputs under the fault [2 1 0]